Biopolymer-reinforced synthetic granular nanocomposites for affordable point-of-use water purification

Mohan Udhaya Sankar[1], Sahaja Aigal[1], Shihabudheen M. Maliyekkal[1], Amrita Chaudhary, Anshup, Avula Anil Kumar, Kamalesh Chaudhari, and Thalappil Pradeep[2]

Unit of Nanoscience and Thematic Unit of Excellence, Department of Chemistry, Indian Institute of Technology Madras, Chennai 600 036, India

Edited by Eric Hoek, University of California, Los Angeles, CA and accepted by the Editorial Board April 4, 2013 (received for review November 21, 2012)

Creation of affordable materials for constant release of silver ions in water is one of the most promising ways to provide microbially safe drinking water for all. Combining the capacity of diverse nanocomposites to scavenge toxic species such as arsenic, lead, and other contaminants along with the above capability can result in affordable, all-inclusive drinking water purifiers that can function without electricity. The critical problem in achieving this is the synthesis of stable materials that can release silver ions continuously in the presence of complex species usually present in drinking water that deposit and cause scaling on nanomaterial surfaces. Here we show that such constant release materials can be synthesized in a simple and effective fashion in water itself without the use of electrical power. The nanocomposite exhibits river sand-like properties, such as higher shear strength in loose and wet forms. These materials have been used to develop an affordable water purifier to deliver clean drinking water at US $2.5/y per family. The ability to prepare nanostructured compositions at near ambient temperature has wide relevance for adsorption-based water purification.

hybrid | green | appropriate technology | frugal science | developing world

Safe drinking water is a significant, but simple indicator of development. Its availability at point of use can save over 2 million human lives (1) (of the 3.575 million deaths caused by water, sanitation, and hygiene issues, 42.6% are due to diarrhea alone: 3.575 million × 0.426 = 1.523 million lives), can avoid over 2 billion diarrheal infections (2), and can contribute over $4 billion to the global gross domestic product (3) (formula used: Σ (number of deaths attributed to diarrhea in each country × corresponding country's per capita gross domestic product). Considering the challenges associated with traditional disinfectants (4), solutions based on state-of-the-art science and technology hold the key for safe drinking water (5) and novel approaches are being looked at (6, 7). It has been long known that silver, especially in nanoparticle form, is an effective disinfectant and works for a wide spectrum of bacteria and viruses (8, 9). Numerous approaches are available for the synthesis of biocidal silver nanoparticles or colloids, including the use of matrices (10–12). The biocidal property of silver nanoparticles, usually in the size range of 10–20 nm, is attributed to the release of trace quantities of silver ions in water (13–16), which, although being sufficient for microorganism killing, does not exhibit toxicity to humans (17, 18). [Toxicity due to silver nanoparticles themselves is also known (16)]. Although a number of silver-based biocidal compositions have been synthesized, those have not been able to reach the masses in large volumes (e.g., silver nanoparticle-loaded ceramic candles) (19). Massive deployment has been hampered due to the following reasons: (*a*) Drinking water contains many species (e.g., inorganic ions and organics) that anchor on the surface of the nanoparticles, making sustained silver ion release difficult (15); (*b*) suitable anchoring substrates that limit the scaling of nanoparticle surfaces while simultaneously preventing their release into water are not available; and (*c*) continued retention of the nanoparticles in the matrix is difficult.

In this work, we demonstrate a unique family of nanocrystalline metal oxyhydroxide-chitosan granular composite materials prepared at near room temperature through an aqueous route. The origin of crystallinity in the composition is attributed to abundant -O- and -OH functional groups on chitosan, which help in the crystallization of metal oxyhydroxide and also ensure strong covalent binding of the nanoparticle surface to the matrix. X-ray photoelectron spectroscopy (XPS) confirms that the composition is rich with surface hydroxyl groups. Using hyperspectral imaging, the absence of nanoparticle leaching in the water was confirmed. Further, a unique scheme to reactivate the silver nanoparticle surface is used for continual antimicrobial activity in drinking waters. Several other composites have been developed that can scavenge other contaminants in water. We demonstrate an affordable water purification device based on such composites developed over several years and undergoing field trials in India, as a potential solution for widespread eradication of the waterborne disease burden.

Results and Discussion

The antimicrobial composition consists of an aluminum oxyhydroxide–chitosan composite (referred to as BM) with silver particles of 10–20 nm diameter embedded in it (Fig. 1*A* and *SI Appendix*, Fig. S1) and is capable of sustained release of silver ions [40 ± 10 parts per billion (ppb)] in natural drinking water over an extended volume of water passing through it, to achieve effective removal of microorganisms (*SI Appendix*, Fig. S2; see Fig. 3*C*). The antimicrobial composite (referred to as Ag-BM) is unique as it is made in water at near room temperature, using a biopolymer, and dried in ambient conditions to obtain water-insoluble granules, yielding Na_2SO_4 as the major by-product (>90%), thereby making it a green synthesis. The concentration of silver ion leached into drinking water from the prepared composite at relevant temperatures (5–35 °C) (*SI Appendix*, Fig. S3) is significantly less than the maximum permissible limit of 100 ppb (secondary standard, US Environmental Protection Agency), thereby requiring no secondary filtration to remove excess silver ions. This controlled release at temperatures of relevance to drinking-water applications over extended periods is an important advantage of the composite. X-ray diffraction patterns of BM and Ag-BM show the presence of

Author contributions: M.U.S., A.C., A., and T.P. designed research; M.U.S., S.A., S.M.M., A.C., A., A.A.K., and K.C. performed research; M.U.S., S.A., A., and T.P. analyzed data; and M.U.S., S.A., A.C., A., and T.P. wrote the paper.

The authors declare no conflict of interest.

This article is a PNAS Direct Submission. E.H. is a guest editor invited by the Editorial Board.

[1]M.U.S., S.A., and S.M.M. contributed equally to this work.

[2]To whom correspondence should be addressed. E-mail: pradeep@iitm.ac.in.

This article contains supporting information online at www.pnas.org/lookup/suppl/doi:10.1073/pnas.1220222110/-/DCSupplemental.

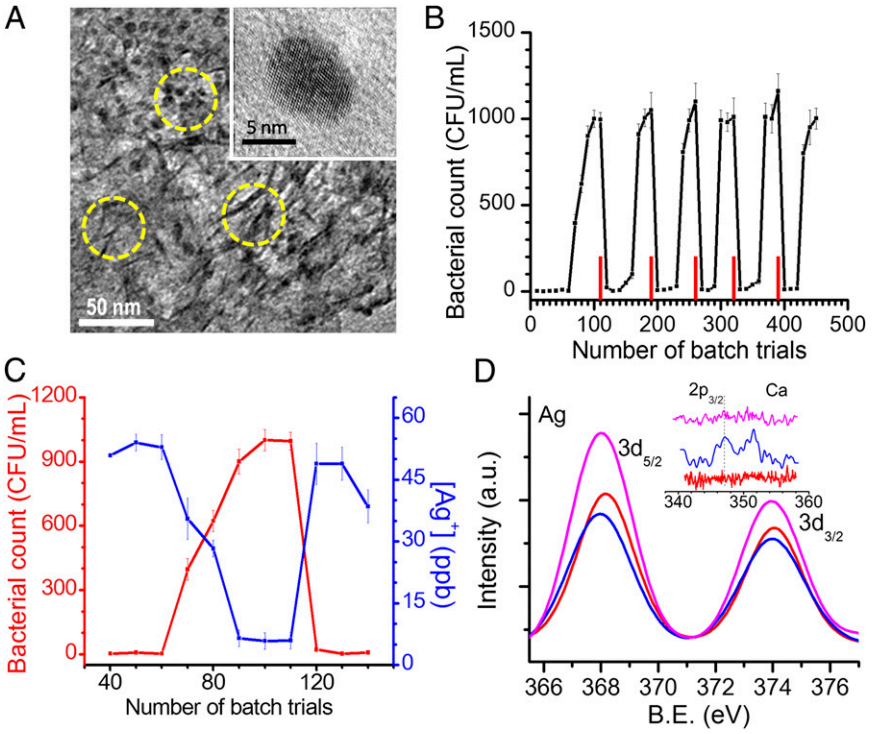

Fig. 1. Characterization of composite and exhibits of its unique antimicrobial activity. (*A*) Transmission electron micrograph of Ag-BM. The composite matrix appears as nanosheets of 3- to 4-nm thickness and the embedded nanoparticles are seen as dots. Some sheets and particles are indicated by circles. The matrix made of the boehmite–chitosan acts like a cage in which the nanoparticles are trapped. The particle sizes are much smaller than those of a typical aqueous phase synthesis. *Inset* shows an expanded view of one particle. (*B*) Bacterial load measured in water as a function of batch upon spiking 10^5 CFU/mL of *E. coli*. Red bars indicate the point of reactivation. (*C*) Silver ion concentration measured by ICP-MS (blue trace) and corresponding bacterial count in CFU/mL for one of the cycles (number of trials: 40th–140th) (red trace) from batch measurements. (*D*) X-ray photoemission spectra of initial (red trace), saturated (blue trace), and reactivated (pink trace) composites in the Ag 3d region and the Ca 2p region (*Inset*). The intensity of Ca 2p (*Inset*) is weak as the coating is thin. The reactivated composite shows an increased Ag 3d intensity due to removal of scale-forming species and better exposure of the nanoparticle surface.

nanocrystalline AlOOH of mean crystallite size of 3.5 nm calculated from the Scherrer formula (*SI Appendix*, Fig. S4).

High-resolution electron micrographs show that the silver nanoparticles are trapped within the AlOOH–chitosan cages, which allow them to be preserved with reduced contact with scale-forming chemical species, yet allowing sufficient interaction with water, due to which sustained release of Ag^+ is possible (Fig. 1*A* and *SI Appendix*, Figs. S1 and S5). The inorganic cages formed by AlOOH are seen as dark lines of 3–4 nm thickness in the transmission electron microscopy (TEM) image and are held together by the chitosan matrix (see below for a discussion of the materials). The nanoparticles are small enough to release Ag^+ and are single crystalline (Fig. 1*A*, *Inset*). This uniformity and reduced particle size are difficult to achieve for silver in a fast, aqueous-phase synthesis.

The composite was tested for antibacterial activity in batch mode (*Materials and Methods*) for more than 400 trials continuously and it exhibited a cyclic pattern of antibacterial action in natural drinking water (Fig. 1*B*). A typical cycle (number of trials: 10th–140th) represents antibacterial performance of Ag-BM at its peak, followed by a drop in performance due to a gradual decrease in Ag^+ release, resulting in an increase in bacterial count in the output water, and finally after reactivation (regaining the ability to leach silver ions) an immediate recovery of performance where Ag^+ release is back to normal (40 ± 10 ppb, Fig. 1*C*).

The concept of reactivation is an important reason behind Ag-BM's long-lasting antimicrobial performance. As seen in Fig. 1*B*, the performance of Ag-BM drops after a certain number of trials (60 trials) due to its continuous exposure to scalants present in water, even though the silver content within the BM matrix is still significant. This drop in performance is explained by studying the XPS of the spent Ag-BM, where the Ag $3d_{5/2}$ peak is at a reduced intensity in comparison with the initial composite (Fig. 1*D*). Factors such as deposition of sparingly soluble species, principally in the form of $CaCO_3$ and silicate precursors, are responsible for the partial filling of the composite with a thin layer of scalants, reducing silver release. The existence of Ca 2p and Si 2p peaks in the XPS spectra of spent Ag-BM proves this (Fig. 1*D*, *Inset* and *SI Appendix*, Fig. S6). SEM-EDAX elemental imaging and spectra also support the presence of deposits containing Ca and Si (*SI Appendix*, Fig. S7). Surface imaging by atomic force microscopy (AFM) shows increased inhomogeneity in the saturated Ag-BM (*SI Appendix*, Fig. S8). The proof of scaling is further substantiated by trials done in natural drinking water and ultrapure water (resistivity: 18 MΩ.cm). In natural drinking water, Ag-BM is subjected to deposition of sparingly soluble species, which limits its efficacy after a period; whereas, due to the nonexistence of these species in ultrapure water, the life of the composite is prolonged and is almost indefinite (*SI Appendix*, Fig. S9). Additionally, the antibacterial efficacy of Ag-BM was tested under prevalent water quality parameters of total dissolved solids (TDS), pH, and total organic carbon (TOC) and performance of the composite was acceptable (*SI Appendix*, Fig. S10). Of the several methods tested, the simplest, most effective, and field implementable one for regaining Ag^+ release is incubating the inactive Ag-BM in water [deionized water or natural drinking water (*SI Appendix*, Fig. S11)] at 70–100 °C for 3–4 h. In a batch experiment, when a finite bacterial colony count (10–50 CFU/mL) was observed in the output, the trials were continued a few more times to ensure the drop in performance and thereafter, the composite was reactivated. The number of trials that can be done after every reactivation slowly reduces with increasing trials. Acid-digested initial Ag-BM showed 0.432% silver by weight, and after 450 trials, it reduced to 0.306%, which corresponds to 71% of Ag still left in the BM matrix. Theoretically, leaching of 29% silver amounts to an average concentration of 50 ppb over 500 batch trials, using 2 g composite. The tests were stopped after 450 trials and Ag-BM was not reactivated further, although the same method may be continued. Innovative reactivation methods may also be used, not limited to the heat treatment method alone (*SI Appendix*, Fig. S12). By using diluted lemon juice, readily available in every home, further reactivation can be done, possibly until the composite gets exhausted completely, i.e., when requisite silver ions cannot be released from the matrix any further.

The composite was tested for antiviral activity in batch mode (*Materials and Methods*) for more than 200 trials continuously in

natural drinking water. The antiviral performance is similar to the antibacterial performance. When the performance deteriorates, the activity is regained after reactivation (*SI Appendix*, Fig. S13).

When a nanocomposite-based approach is used for drinking-water purification, the possibility of nanoparticle release in drinking water exists. To confirm the effective trapping of nanoparticles in the matrix and absence of any observable nanoparticle release in water, dark-field microscopy was done on the bacteria. Microscopic images (Fig. 2 and *SI Appendix*, Figs. S14 and S15) show that although nanoparticles are seen within the bacterial contour of citrate-protected Ag nanoparticle-treated bacterial cells, no nanoparticle is seen in bacterial cells treated with Ag-BM. However, lysis is observed in both cases as observed in the discontinuity of the cell membrane (Fig. 2 *B* and *C* and 2 *D* and *E*, *Insets*). The hyperspectral images of bacterial cells treated with citrate-protected Ag nanoparticles show distinct size-dependent surface plasmon features of the nanoparticles (Fig. 2*D*) that are absent in the case of Ag-BM–treated bacterial cells (Fig. 2*E*). The data conclusively established that silver ions released from Ag-BM are responsible for the antibacterial activity and there is no observable nanoparticle release in water. It is also confirmed that during the interaction of water with the composition, AlOOH–chitosan does not undergo dissolution; aluminum release in water is less than 6 ppb (aluminum secondary standard: 50–200 ppb, US Environmental Protection Agency) and total organic carbon is nearly 0.1 ppm (*SI Appendix*, Fig. S16). Independent spectroscopic measurements of Ag-BM–treated water samples and the cyclic nature of antibacterial performance also support this. The antibacterial activity of Ag-BM was also shown by fluorescence microscopy study of treated bacteria where a mixture of nucleic acid-binding fluorescent dyes [green fluorescent SYTO9 dye and red fluorescent propidium iodide (PI) dye] were used (*SI Appendix*, Fig. S17).

A water purification device (Fig. 3 *A* and *B*) containing 50 g of Ag-BM in cartridge form was assessed for performance under standard test conditions. This filter ran up to 1,500 L with a bacterial input load of 10^5 CFU/mL without the need for reactivation (Fig. 3*C* and *SI Appendix*, Fig. S2). Therefore, by using 120 g composite, safe drinking water can be provided for a family of five for 1 y (assuming daily drinking water consumption of 10 L). This translates to an annual expense of $2 per family. (Cost of media, sediment prefilter, plastic assembly, and cartridge packing are included in the cost calculation.) By reactivating this composite, the life of the cartridge can be enhanced further, thereby reducing the cost. The water purification device has a second-stage axial filtration based on an activated carbon block (Fig. 3*A*) with a nominal pore size of <4 μm, which enables it to remove cysts through physical filtration, and the cyst removal capacity is higher than 5 log (input count, 10^6 particles per liter; output count, <3 particles per liter), in accord with the National Science Foundation (NSF) protocol P231 (*SI Appendix*, Fig. S18). The carbon block has an additional function of removing any organic and bacterial biomass as well, besides removing traces of silver ions or silver bound with microbial debris. However, residual silver ion content may be advantageous in some cases to prevent microbial contamination in water upon storage as well as to prevent bio-fouling of the composite during periods of nonuse.

Considering the fact that some parts of the world have severe chemical contamination in ground water (20), causing life-threatening diseases, suitable unique composites may be packed into the carbon filter to remove harmful chemical contaminants such as arsenic, pesticides, mercury, lead, iron, etc., so that chemically and microbiologically pure water is obtained, depending on the region of use. Composite preparation at room temperature is crucial for addressing health-related contaminants as the method preserves active adsorption sites (for example, surface hydroxyl groups undergo dehydration on exposure to higher temperature).

For example, to remove iron, 100 g iron oxyhydroxide–chitosan composite (*Materials and Methods*) was taken. Feed water containing freshly prepared 5 ± 1 ppm of Fe^{2+} was passed through the composite at a flow rate of 50 mL/min. The output water was tested for both Fe^{3+} and Fe^{2+} by spectrophotometric methods. The column was run for 1,500 L and the output concentration was consistently below 0.3 ppm, thereby adhering to the World Health

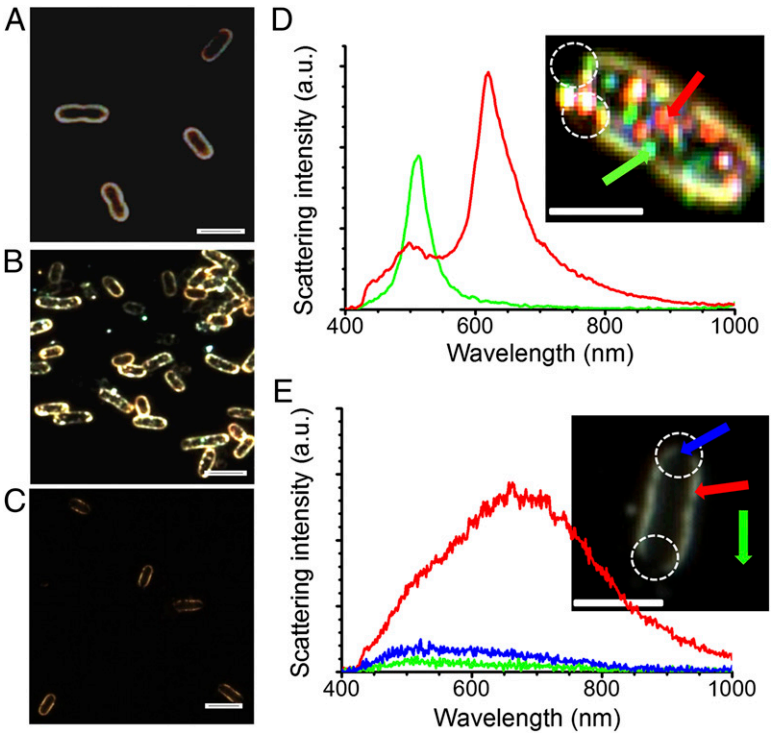

Fig. 2. Microscopic examination of bacterial lysis through dark-field and hyperspectral imaging. (*A*–*C*) Dark-field microscopy images of bacteria in water, bacteria treated with citrate-protected Ag nanoparticles, and bacteria treated with Ag-BM, respectively. (*A*) Continuous bacterial contour. (*B*) Nanoparticles within and outside the bacterial contour, which are seen as bright dots. (*C*) Discontinuous bacterial contour with the absence of nanoparticles from Ag-BM. (*D*) Scattering spectra of single nanoparticles embedded in the bacterial contour. (*Inset*) Hyperspectral image from which the spectra are taken. The spectral traces and the arrows correspond to the same particles. (*E*) Scattering spectra of lysed bacterial border after treating with Ag-BM. *Inset* shows the hyperspectral image of a bacterium treated with Ag-BM. The color of the traces and the points from which spectra are collected (shown by arrows) are the same. Blue and green traces in *E* are nearly the same, indicating that the lysed regions appear like background. Lysis is shown by white circles in the images in *D* and *E*. (Scale bars in all images: 2 μm.) Scattering from nanoparticles is approximately an order of magnitude larger compared with the bacterial contour.

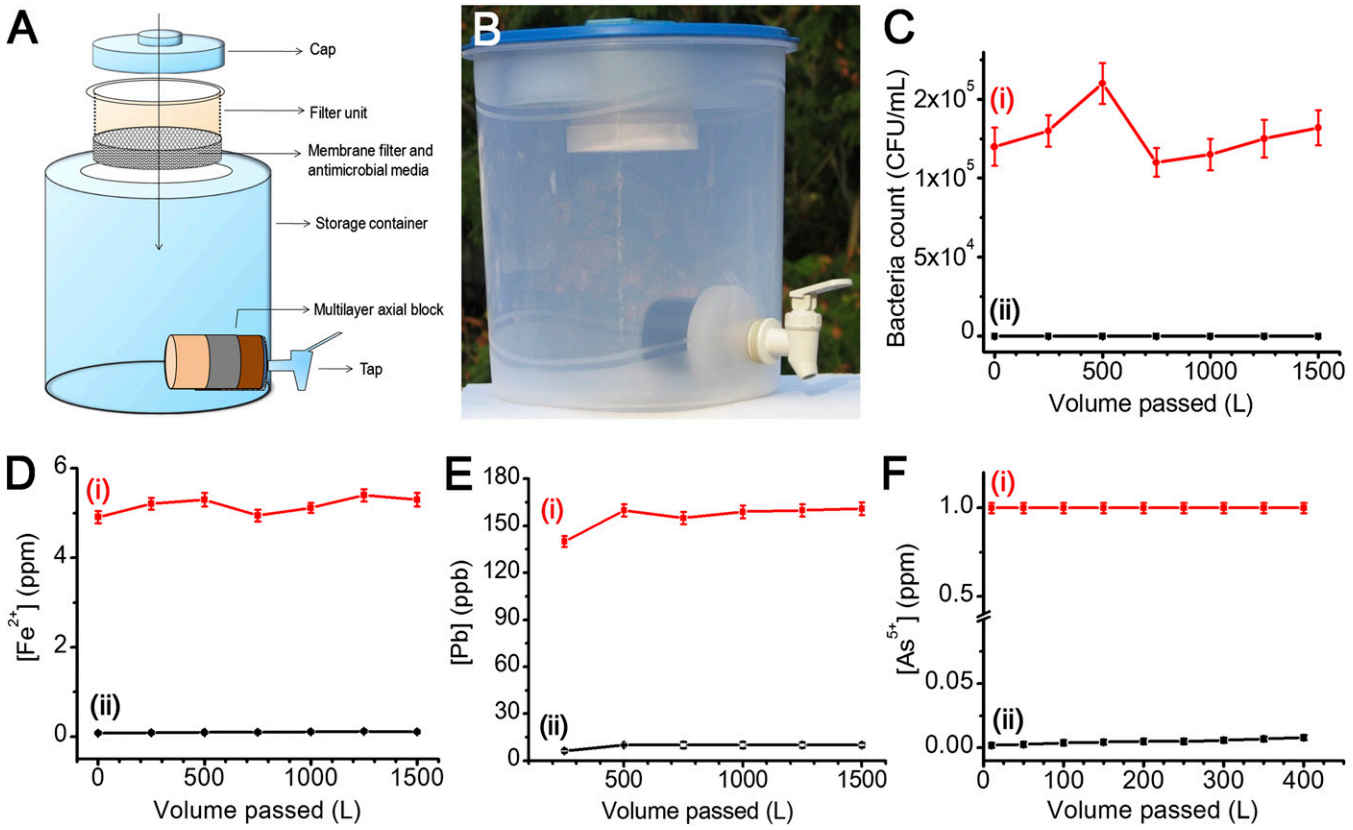

Fig. 3. Water purification device undergoing field trials in India and its performance evaluation. (*A*) Schematic diagram of the device. (*B*) Actual photograph of the device. Construction and assembly of the device are simple and can be done locally. The antimicrobial composition is used as granules and kept in the membrane filter. Carbon block is positioned just before the tap. Carbon block may also be used as a multilayer axial block, comprising adsorbents for specific regional contaminants such as arsenic, iron, and lead. (*C–F*) Column data for the removal of (*C*) *E. coli*, (*D*) Fe^{2+}, (*E*) Pb^{2+}, and (*F*) As^{5+}. Input (*i*) and output (*ii*) concentrations are indicated in *C–F*.

Organization (WHO) norms (Fig. 3*D*). Similarly, to remove lead, 50 g of nano-MnO_2–loaded BM composite was packed in a column and fed with 1,500 L of water spiked with 150 ± 10 ppb of Pb^{2+}. The total concentration of lead in the output water (Pb exists in ionized as well as hydrolyzed form at the pH of drinking water), measured by inductively coupled plasma mass spectrometry (ICP-MS), was consistently below 10 ± 1 ppb, adhering to the WHO norms (Fig. 3*E*). Additionally, arsenic mitigation from drinking water was effectively carried out using iron oxyhydroxide–chitosan composite. Twenty grams of granular composite was packed in a column and fed with 400 L of water spiked with 1 ppm of arsenic (As^{5+}) at a flow rate of 50 mL/min. Total arsenic concentration in the output water, measured by ICP-MS, was less than 10 ppb, below the permissible limit (Fig. 3*F*). Similar performance was seen with an input As^{3+} concentration of 1 ppm. Please note that the input concentrations were the maximum concentrations usually encountered in the field. The carbon block shown in Fig. 3 *A* and *B* may also be used as a multilayer axial block, comprising the above adsorbents for specific regional contaminants such as arsenic, iron, and lead.

To use the composition in a water purification cartridge, it is important that it has satisfactory wet strength to stay intact as a granular composition. Compositions that are obtained as powders offer poor hydraulic conductivity, leading to excessive pressure drop in the water purification cartridge operated with gravity pressure. To find the shear strength of the granular media, a direct shear test was conducted at different normal stresses. The maximum horizontal shear stress exhibited by the iron oxyhydroxide–chitosan composite under each normal stress is shown in *SI Appendix*, Fig. S19 *A* and *B*. These data are plotted in *SI Appendix*, Fig. S20 *A* and *B*. Straight-line approximation of the Mohr–Coulomb failure pattern gave the angle of internal friction (Φ) to be 41.76° and 44.07° for dry and wet media, respectively, showing that the prepared granular media's shear strength is equivalent to that of the Indian standard sand (~35–40°). The compressive strength of the iron oxyhydroxide–chitosan composite was found to be 25 MPa, comparable to that of concrete.

The essence of the approach to prepare the composition is described graphically in Fig. 4. Al^{3+}-complexed chitosan solution (pH 0.8) was treated with an alkali (Fig. 4 *A*, *ii*). Alkali treatment initiates aluminum ion hydrolysis (leading to the formation of aluminum hydroxide nanoparticles) followed by chitosan precipitation (random coiled water-insoluble chitosan network) (Fig. 4 *A*, *iii*). Fig. 4*B* shows photographs of aluminum hydroxide in the dispersed form at a solution pH 4–6 and settled residue of aluminum hydroxide–chitosan at pH 7 and above. Generally, Al^{3+} upon alkaline hydrolysis converts to an aluminum hydroxide gel and prolonged heating of the gel to temperatures above 80 °C leads to redissolution of aluminum hydroxide and subsequent crystallization to aluminum oxyhydroxide. Abundant -O- and -OH groups of chitosan act as nucleation centers for the formation of boehmite nanocrystals and this crystallization is promoted even at room temperature. There are crucial advantages associated with boehmite crystallization at room temperature: (*i*) Surface hydroxyl concentration stays highest whereas exposure to elevated temperature causes their destruction, thereby giving reduced adsorption capacity, and (*ii*) reduced production cost as heating can be avoided completely.

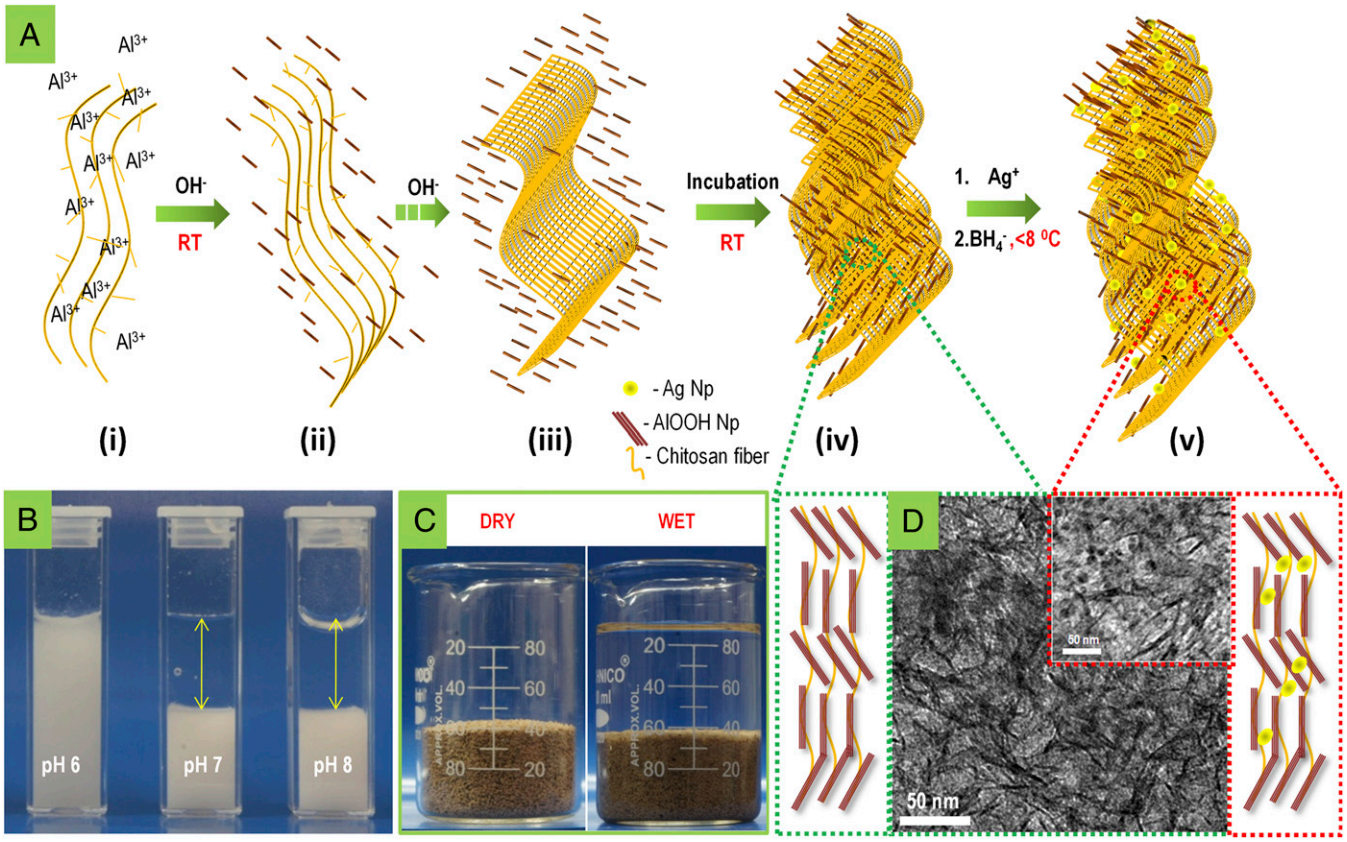

Fig. 4. Mechanism for the preparation of composite and origin of its physical strength in water due to network structure. (*A*) Mechanistic scheme for the formation of Ag-BM composite, as learned through various experiments. (*i–v*) (*i*) Al^{3+} complexes with chitosan solution; (*ii* and *iii*) alkali treatment leads to formation of aluminum hydroxide nanoparticles and random coiled chitosan network; (*iv*) aluminum hydroxide nanoparticles bind to chitosan network, possibly through covalent sharing of oxygen, leading to the formation of aluminum oxyhydroxide; and (*v*) silver nanoparticles form on the aluminum oxyhydroxide–chitosan network. (*B*) Photographs of the system during synthesis. Presence of aluminum hydroxide in the supernatant is clearly visible below pH 6 whereas bound aluminum hydroxide settles at pH 7 and pH 8, leading to a clear supernatant. (*C*) Photographs of the composite granules and of the same in water to illustrate that the material is stable in water. (*D*) Graphical representation and corresponding TEM images showing the aluminum oxyhydroxide-chitosan network without (green box) and with (red box) embedded silver nanoparticles.

We have observed that chitosan has the ability to bind colloidal nanoparticles in a proportion higher than 500 wt/wt% (Fig. 4 *A*, *iv*). Note that the role of chitosan is not merely as a flocculating agent for the precipitation of colloidal nanoparticles. In flocculation, colloidal particles undergo charge neutralization while binding with the flocculating agent. As a consequence, there is a reduction in the capacity to remove charge-bearing contaminants (such as arsenic or fluoride). However, the heavy metal ion-binding capability of aluminum oxyhydroxide–chitosan vis-à-vis equivalent chitosan is similar (Zn^{2+} binding ability: 53 mg/g and 56 mg/g, respectively, at an equilibrium concentration of 50 ppm). This means that functional groups for metal ion binding are largely available, even after hydrolysis of aluminum. A covalent interaction between chitosan and AlOOH ensures that charged sites on AlOOH are available for ion adsorption. Please note that typical sites on an oxide surface are MOH, MOH_2^+, and MO^-, with respective fractions determined by the pH.

Chitosan and AlOOH synergistically participate in the structural integrity of the composite. Chitosan undergoes swelling in water, due to destruction of hydrogen bonding. This behavior is similar to that observed in cellulose. Similarly, AlOOH disintegrates into finer particles upon exposure to water. However, the nanoscale AlOOH–chitosan composite, having a molecular-scale interaction of the individual components, does not exhibit any sign of disintegration in water. We propose that chitosan reinforces the AlOOH structure and vice versa, which imparts exceptional stability and strength to the composite in water (Fig. 4*C*). This molecularly assembled AlOOH–chitosan composite, exhibiting a cage-like structure, plays a critical role in stabilizing the silver nanoparticles (schematically illustrated in Fig. 4*D*). Upon addition of silver ions to AlOOH–chitosan, chitosan binds with silver due to its heavy metal ion-binding capacity. Upon addition of $NaBH_4$, silver ions reduce to zero valent nanoparticles, which are trapped in the AlOOH–chitosan cages (Fig. 4*A*, *v*). The presence of silver nanoparticles in the cage ensures their stabilization, while decreasing their exposure to scalants simultaneously, allowing release of silver ions in natural drinking water.

Conclusions

In their entirety, the proposed device and materials present a compelling solution for achieving the United Nations millennium development goal of sustainable access to safe drinking water. We believe that frugal science (21) based on nanotechnology can make a lasting impact on society. There are over 200 million households in India. Dissemination of this technology in various forms such as cartridges, sachets, etc., can generate large employment opportunities in the villages. The production of composites and water filter devices and their deployment and servicing can contribute to the local economy. Various modifications of the composite with different compositions have been developed with comparable performances.

Materials and Methods

The granular composites, composed of metal oxyhydroxide–chitosan nanostructures, were synthesized by a green synthetic route, which in general comprises hydrolysis of a metal precursor–chitosan complex using an alkaline medium followed by washing and drying at ambient conditions. Metal ion precursors that may be used for the preparation of composites are Al^{3+}, Fe^{3+}, Fe^{2+}, Mn^{2+}, Cu^{2+}, Zn^{2+}, Ti^{4+}, and Ce^{4+}. All syntheses were carried out in water.

Synthesis of the Composite for Bacteria and Virus Removal. An aluminum oxyhydroxide–chitosan nanostructure embedded with silver nanoparticles was synthesized by a two-step process: (*i*) Synthesis of the aluminum oxyhydroxide–chitosan nanostructure (referred to as BM): 1.5 g chitosan was dissolved in 0.5% nitric acid solution and to this mixture, 100 mL of 0.5 M aluminum sulfate was added dropwise. After 3 h incubation, 140 mL of 2 M sodium hydroxide was added dropwise to precipitate aluminum and chitosan. The resultant precipitate was further stirred for 1 h and subsequently washed with copious amounts of water. This precipitate is called BM. (*ii*) Synthesis of silver nanoparticle in BM: After redispersing the precipitate in water, 100 mL of 5 mM silver nitrate was added and incubated for 1 h. Afterwards, 100 mL of 10 mM sodium borohydride was added dropwise at <10 °C and the mixture was stirred continuously. The final precipitate was subsequently washed with copious amounts of water, dried at room temperature (28–30 °C), crushed, and used for further studies. The resulting composite was insoluble in water and appears as light yellow granules, referred to as Ag-BM. The method of composite preparation is water positive by two to three orders of magnitude; i.e., it produces 500 L of clean water for every 1 L of water consumed for material production.

Synthesis of Composite for Heavy Metal Removal. An aluminum oxyhydroxide–chitosan nanostructure embedded with nano-MnO_2 particles was synthesized through a two-step process: (*i*) synthesis of BM and (*ii*) MnO_2 nanoparticles incorporation in BM. Briefly, after redispersing the BM precipitate in water, a freshly prepared MnO_2 nanoparticles suspension was added dropwise and the mixture was stirred continuously. The final precipitate was subsequently washed with copious amounts of water, dried at room temperature, crushed, and used for further studies. The resulting composite was insoluble in water and appeared as black granules.

Synthesis of Composite for Arsenic and Iron Removal. The iron oxyhydroxide–chitosan nanostructure was prepared by the route described in *Synthesis of Composite for Bacteria and Virus Removal* for the preparation of BM. Ferric sulfate was used as the metal ion precursor for iron. The final precipitate was dried at room temperature, crushed, and used for further studies. The resulting composite was insoluble in water and appeared as brown granules.

Synthesis of Silver Nanoparticles for Hyperspectral Imaging. Silver nanoparticles used for hyperspectral imaging (HSI) are prepared through $NaBH_4$ reduction method. $AgNO_3$ (1 mM) was mixed with 1 mM trisodium citrate solution in equal volumes. An equal volume of 10 mM ice-cooled solution of $NaBH_4$ was then added dropwise to the above solution with stirring. The solution turns golden yellow and exhibits an absorption maximum at 390 nm, corresponding to an average particle diameter of 5–10 nm.

Testing protocol for antibacterial and antiviral efficacy. Two grams of Ag-BM was shaken with 100 mL of natural drinking water (see *SI Appendix*, Table S1 for water quality parameters). Antibacterial activity of Ag-BM was measured by spiking the natural drinking water with *Escherichia coli* (*E. coli* ATCC 25922) at a concentration of $\sim 1 \times 10^5$ CFU/mL, whereas antiviral activity was measured by spiking the water with bacteriophage MS2 at a concentration of $\sim 1 \times 10^3$ PFU/mL. Thereafter, the water was left standing for 1 h and subsequently the surviving microorganism count was measured by conventional pour plate (*E. coli*) and plaque assay (bacteriophage MS2) techniques. Colony counts were performed after incubation at 37 °C for 48 h (*E. coli*) and 16 h (bacteriophage MS2). It should be noted that the input bacteria and virus concentration may vary slightly in studies extending for weeks as the cultures are prepared on a daily basis.

Testing protocol for the water purification device. For the water purification device studies, 50 g of the composite was packed in a water purification cartridge (diameter, 70 mm; height, 2 mm) and assembled as a gravity-fed water purifier. The feed water was passed at a flow rate of 1,000 mL/min. The input tap water was periodically subjected to a bacterial load of $\sim 1 \times 10^5$ CFU/mL and the output water was plated in accordance with the protocol to understand the biocidal performance activity. Cyst removal studies were conducted following the NSF protocol P231 and NSF/American National Standards Institute standard 53. Polystyrene beads with a nominal size of 4–6 μm were used as a surrogate for cysts. An input concentration of $\sim 1 \times 10^6$ particles per liter was passed through the carbon block. Input and output concentrations were directly examined by a scanning electron microscope. Output water was concentrated ×1,000 before examination.

Details of the fluorescence microscopy protocol, mechanical testing of composite, and material characterization techniques used in this study are described in *SI Appendix, Methods* and *SI Appendix, Material Characterization*.

ACKNOWLEDGMENTS. We thank M. S. Bootharaju, S. Banupriya, P. R. Sajanlal, Robin John, and Rakhil Akkali for their technical support in conducting X-ray photoelectron spectroscopy, transmission electron microscopy, field emission scanning electron microscopy, atomic force microscopy, and fluorescence microscopy measurements, respectively. We thank Dr. R. G. Robinson and Dr. Manu Santhanam (Department of Civil Engineering) for their technical support in direct shear test and compressive strength analyses. We thank the Department of Science and Technology (Government of India) for constantly supporting our research program on nanomaterials.

1. Prüss-Ustün A, Bos R, Gore F, Bartram J (2008) *Safer Water, Better Health* (WHO, Geneva).
2. Clasen TF, Haller L (2008) *Water quality interventions to prevent diarrhoea: Cost and cost-effectiveness* (WHO, Geneva).
3. (2004) *The World Factbook 2004* (Central Intelligence Agency, Washington, DC).
4. Sedlak DL, von Gunten U (2011) Chemistry. The chlorine dilemma. *Science* 331(6013): 42–43.
5. Shannon MA, et al. (2008) Science and technology for water purification in the coming decades. *Nature* 452(7185):301–310.
6. (2009) *Nanotechnology Applications for Clean Water*, eds Savage N, et al. (William Andrew Publication, Norwich, NY).
7. Kim SJ, Ko SH, Kang KH, Han J (2010) Direct seawater desalination by ion concentration polarization. *Nat Nanotechnol* 5(4):297–301.
8. Pradeep T, Anshup (2009) Noble metal nanoparticles for water purification: A critical review. *Thin Solid Films* 517(24):6441–6478.
9. De Gusseme B, et al. (2010) Biogenic silver for disinfection of water contaminated with viruses. *Appl Environ Microbiol* 76(4):1082–1087.
10. Kumar A, Vemula PK, Ajayan PM, John G (2008) Silver-nanoparticle-embedded antimicrobial paints based on vegetable oil. *Nat Mater* 7(3):236–241.
11. Dai J, Bruening ML (2002) Catalytic nanoparticles formed by reduction of metal ions in multilayered polyelectrolyte films. *Nano Lett* 2(5):497–501.
12. Jain P, Pradeep T (2005) Potential of silver nanoparticle-coated polyurethane foam as an antibacterial water filter. *Biotechnol Bioeng* 90(1):59–63.
13. Liu J, Hurt RH (2010) Ion release kinetics and particle persistence in aqueous nanosilver colloids. *Environ Sci Technol* 44(6):2169–2175.
14. Kittler S, Greulich C, Diendorf J, Köller M, Epple M (2010) Toxicity of silver nanoparticles increases during storage because of slow dissolution under release of silver ions. *Chem Mater* 22(16):4548–4554.
15. Jin X, et al. (2010) High-throughput screening of silver nanoparticle stability and bacterial inactivation in aquatic media: Influence of specific ions. *Environ Sci Technol* 44(19):7321–7328.
16. Marambio-Jones C, Hoek EMV (2010) A review of the antibacterial effects of silver nanomaterials and potential implications for human health and the environment. *J Nanopart Res* 12(5):1531–1551.
17. Nowack B (2010) Chemistry. Nanosilver revisited downstream. *Science* 330(6007): 1054–1055.
18. Berger TJ, Spadaro JA, Chapin SE, Becker RO (1976) Electrically generated silver ions: Quantitative effects on bacterial and mammalian cells. *Antimicrob Agents Chemother* 9(2):357–358.
19. Franz AM (2004) A *performance* study of ceramic candle filters in Kenya including tests for coliphage removal (Massachusetts Institute of Technology, Cambridge, MA). Available at http://dspace.mit.edu/bitstream/handle/1721.1/31120/61162474.pdf.
20. Qiu J (2011) Environmental science. China to spend billions cleaning up groundwater. *Science* 334(6057):745.
21. Whitesides G (2011) The frugal way: The promise of cost-conscious science. *The World in 2012*, ed, Franklin D, The Economist, pp 154.